Universität Stuttgart

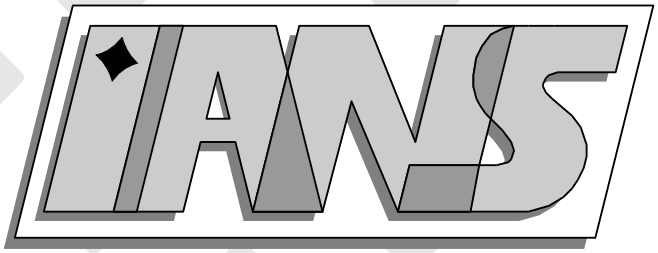

Investigation of heat generation by acoustic waves

M. Kaltenbacher, I. Shevchenko, B. Wohlmuth

Berichte aus dem Institut für Angewandte Analysis und Numerische Simulation

Documentation 2010/001

Universität Stuttgart

Investigation of heat generation by acoustic waves

M. Kaltenbacher, I. Shevchenko, B. Wohlmuth

Berichte aus dem Institut für Angewandte Analysis und Numerische Simulation

Documentation 2010/001

Institut für Angewandte Analysis und Numerische Simulation (IANS)
Fakultät Mathematik und Physik
Fachbereich Mathematik
Pfaffenwaldring 57
D-70 569 Stuttgart

E-Mail: ians-preprints@mathematik.uni-stuttgart.de
WWW: http://preprints.ians.uni-stuttgart.de

ISSN **1611-4176**

Abstract

We present a numerical scheme for the efficient simulation of isotropic media heating by acoustic waves using a multi-time stepping integration method. The application of the method is dictated by the different time-scales in which the temperature and the acoustic fields evolve. The two-dimensional governing equations based on a modified Pennes bioheat transfer model and a nonlinear wave equation with a temperature dependent speed of sound as well as Kuznetsov's wave equation are discretized in space by finite elements, whereas for the time integration a multi-time stepping technique based on the generalized α-method is proposed. In this model, we are faced with the problem where the wave is propagated through an unbounded domain which is modeled by absorbing boundary conditions on a bounded region. We use the second order Engquist–Majda boundary conditions which are incorporated into the weak formulation of the original problem in terms of Lagrange multipliers. Numerical simulation results show that the multi-time stepping method is efficient and makes calculations of both acoustic waves propagation at high frequencies and heat transfer process in the time-domain feasible.

Key words: Pennes bioheat equation, temperature dependent speed of sound, Kuznetsov's equation, Engquist–Majda absorbing boundary conditions, finite element method, Lagrange multipliers, generalized α-method, multi-time stepping method.

Introduction

Many branches of modern medicine, e.g. cryotherapy, laser surgery and cancer hyperthermia, require the understanding of heat transfer phenomenon in biotissues. The creation of controlled temperature fields in the deep-seated biological tissues by endocavity ultrasound applicators is not only a question of special field-oriented medical instruments but also an actual and challenging research topic of mathematical modeling. The heating of media by ultrasound waves offers a desirable effect for a variety of applications. For instance, the noninvasive ultrasonic thermotherapy of cancer in which destruction of soft tissue in the body is effected through high temperatures generated by local absorption of wave energy.

Acoustic hyperthermia is a phenomenon occurring due to absorption of wave energy by internal tissues. Generally, the nonlinear Kuznetsov equation is used to describe wave propagation [14] while the process of heat transfer in biological systems can be modeled by the equation generally known either as the bioheat equation or as the Pennes equation [21]. In this study, we concentrate not on the bioheat transfer model itself but on the numerical methods for the ultrasonic heating problem. Because of that we modify the Pennes equation by neglecting the blood perfusion and metabolic activity terms.

Usually, the simulation of wave propagation assumes introducing artificial boundaries to limit the computational region. Such idealized boundaries impose tight restrictions on the boundary conditions in order to guarantee a well-posed solution to the differential equation as well as to minimize unphysical artificial reflections which occur at the boundaries. A large variety of non-reflecting boundary conditions has been developed since the 1970s [1, 2, 8, 10, 11, 13, 18]. In the considered model, the well-known second order Engquist–Majda absorbing boundary condition (ABC) is employed [8]. We also discuss how to incorporate the ABC into the weak formulation of the original problem through a Lagrange multiplier approach.

As it is well known, the wave propagation and heat conduction are processes which occur in different time scales. The temperature field evolves quite slowly and can be fully resolved in the range of seconds. On the contrary, the ultrasound waves are emitted with frequencies ranged from 100 kHz to 10 MHz that even the lowest frequency wave may require millions of time steps per second to be resolved. That makes the time scales incomparable and requires special attention being paid to numerical methods for such kind of problems. Usually, such numerical techniques use a transient simulation for the temperature field and solve the acoustic equation in the frequency domain that restricts the applicability of the method to the linear wave equation. However, a more realistic model takes also into account non-linear effects and the distortion of both density

and speed of sound when studying wave propagation and acoustically induced heat conduction process [16, 17, 19].

A time-domain simulation of the ultrasonic heating problem is a very resources consuming task due to the big discrepancy in time scales of the wave propagation and heat conduction processes. One possibility is to use multi-time stepping methods allowing to solve both equations in different time scales. In this paper, we implement a multi-time integration method making calculations in reasonable time.

This rest of the paper is organized as follows. The problem definition is given in Section 1, and we devote Section 2 to the discretization of the original model and to the weak formulation of the second order ABC. Then a multi-time stepping integration method is developed in Section 3. Numerical tests illustrating the validity of the proposed approach and the numerical simulation of a practical application are given in Section 4.

1 Governing equations

The mathematical description of heat transfer in biotissues starts from the nonlinear model of acoustic wave propagation in absorbing media and the heat conduction equation equipped with a source term [4, 20] in the form of total wave energy averaged over time. The source term plays a part of a connecting link coupling acoustic and temperature fields.

We consider a computational domain $\Omega \subset \mathbb{R}^2$ as shown in Fig.1. The computational region is

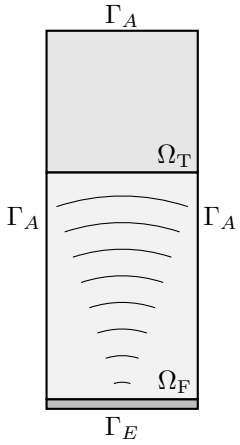

Figure 1: Geometrical setup for the coupled ultrasonic-heating problem

divided into two subdomains: Ω_{F} is a subregion filled up with a fluid and Ω_{T} is a biotissue region whereas the acoustic wave propagation domain is $\Omega = \Omega_{\mathrm{F}} \cup \Omega_{\mathrm{T}}$. The emitter is modeled by the corresponding boundary conditions of the wave equation.

1.1 Nonlinear acoustic wave equation

In the following description, we are guided by two acoustic wave propagation equations: a nonlinear equation with a temperature dependent speed of sound and Kuznetsov's equation for the scalar velocity potential ψ which is related to the acoustic pressure p_a and the acoustic velocity field $\mathbf{v}_a$, by means of $p_a = \rho_a \dot{\psi}$ and $\mathbf{v}_a = -\nabla\psi$. According to [19] a nonlinear wave equation in Ω with a temperature dependent speed of sound is

$$\frac{1}{c^2(T)}\ddot{\psi} + \dot{\psi}\frac{\partial}{\partial t}c^{-2}(T) = \Delta\psi \quad \text{in } \Omega \times (0, t_n). \tag{1.1}$$

Following the paper [14], nonlinear sound waves within the domain Ω are governed by the Kuznetsov equation

$$\frac{1}{c^2}\ddot{\psi} - \triangle\psi = \frac{1}{c^2}\frac{\partial}{\partial t}\left(b\triangle\psi + \frac{1}{c^2}\frac{B}{2A}\dot{\psi}^2 + (\nabla\psi)^2\right) \quad \text{in } \Omega \times (0, t_n). \tag{1.2}$$

Both equations are equipped with Neumann

$$\frac{\partial\psi}{\partial\mathbf{n}} = g(t) \quad \text{on } \Gamma_E \times (0, t_n), \tag{1.3}$$

and the following first

$$\frac{\partial\psi}{\partial\mathbf{n}} + \frac{1}{c}\dot{\psi} = 0 \quad \text{on } \Gamma_A \times (0, t_n), \tag{1.4}$$

or second order

$$\frac{1}{c}\frac{\partial\dot{\psi}}{\partial\mathbf{n}} + \frac{1}{c^2}\ddot{\psi} - \frac{1}{2}\psi_{\tau\tau} = 0 \quad \text{on } \Gamma_A \times (0, t_n). \tag{1.5}$$

Engquist–Majda absorbing boundary conditions.

For equations (1.1) and (1.2) the initial conditions have the form

$$\psi(\cdot, t = 0) = \psi_0, \ \dot{\psi}(\cdot, t = 0) = \psi_1 \quad \text{in } \Omega. \tag{1.6}$$

Here T is the temperature, c is the speed of sound, parameter b accounts for absorption in the media due to viscosity and thermal conductivity, B/A denotes the nonlinearity parameter for the fluid. The subscript τ stands for the tangential derivative of the corresponding function on Γ_A, $\dot{\psi}$ and $\ddot{\psi}$ are the first and second order derivatives with respect to time and $\mathbf{n}$ is the unit normal vector on boundary Γ_A pointing outward Ω.

1.2 Linear acoustic wave equation

The linear acoustic wave propagation can be easily obtained from the Kuznetsov equation (1.2) by setting its right hand side to zero. Thus we have

$$\frac{1}{c^2}\ddot{\psi} - \triangle\psi = 0 \quad \text{in } \Omega \times (0, t_n). \tag{1.7}$$

Despite the importance of treating nonlinear wave equations (1.1) and (1.2), we also consider their linear analog for further comparison of ABCs (1.4)-(1.5) and how they influence the wave propagation.

1.3 Thermal model

The thermal model of interest can be derived from the Pennes equation by a truncation of the blood perfusion and metabolic activity terms. Thus the problem of heat transferring read as follows: for a given temperature T_0 find $T : \Omega \times (0, t_n) \to \mathbb{R}$ satisfying the equation

$$\rho(T)c_\nu\dot{T} = \kappa\Delta T + \langle q \rangle \tag{1.8}$$

with the homogeneous Dirichlet boundary condition

$$T = 0 \quad \text{on } \Gamma_A \cup \Gamma_E \times (0, t_n), \tag{1.9}$$

and the initial condition

$$T(\cdot, t = 0) = T_0 \quad \text{in } \Omega. \tag{1.10}$$

The parameter c_ν is the specific heat capacity, κ is the thermal conductivity, ρ is the temperature dependent density. The acoustic source term q is the total acoustic energy absorbed and converted to heat, i.e. $q = -\nabla \cdot \mathbf{I}$ with $\mathbf{I} = p_a\mathbf{v}_a$ standing for the sound wave intensity. In terms of the acoustic potential the source term is $q = \rho_0(\nabla\dot{\psi} \cdot \nabla\psi + \dot{\psi}\Delta\psi)$, where ρ_0 is the mean density.

The source term was firstly obtained by Nyborg [20] and later in [4], and valid for arbitrary wave propagation. Here $\langle q \rangle$ stands for temporal average of q. We remark that this temporal averaging must be performed over a sufficiently long time interval within which the wave does not change its general character.

2 Discretization

In this section, we derive a weak formulation and finite element discretization for both the linear and nonlinear acoustic equations with the first and second order ABCs as well as for the thermal model. Furthermore, we consider a scheme allowing to incorporate the second order ABCs into the weak formulation.

2.1 Weak formulation of the Engquist–Majda ABCs

The weak formulation of equation (1.7) equipped with the first order ABCs can be constructed by multiplying it with a test function ϕ and then integrating over the problem region. Find the map $\psi(\cdot, t) : \Omega \times (0, t_n) \to \mathbb{R}$ such that

$$\int\limits_{\Omega} \frac{1}{c^2}\ddot{\psi}\phi \; d\Omega + \int\limits_{\Omega} (\nabla\psi \cdot \nabla\phi) \; d\Omega - \int\limits_{\Gamma_A} \phi\nabla\psi \cdot \mathbf{n} \; d\Gamma_A - \int\limits_{\Gamma_E} \phi\nabla\psi \cdot \mathbf{n} \; d\Gamma_E = 0 \quad \text{in } \Omega \times (0, t_n). \tag{2.1}$$

In an overwhelming majority of applications unbounded domains are required that demands ABCs. To fulfill those requests we use the absorbing boundary Γ_A on which we set condition (1.4). The equivalence of the normal derivative to the term $\nabla\psi \cdot \mathbf{n}$ allows to rewrite (2.1) in the form with condition (1.4) and further using (1.3) results in

$$\int\limits_{\Omega} \frac{1}{c^2}\ddot{\psi}\phi \; d\Omega + \int\limits_{\Omega} (\nabla\psi \cdot \nabla\phi) \; d\Omega + \int\limits_{\Gamma_A} \frac{1}{c}\phi\dot{\psi} \; d\Gamma_A - \int\limits_{\Gamma_E} \phi g \; d\Gamma_E = 0 \quad \text{in } \Omega \times (0, t_n). \tag{2.2}$$

As it can be seen from (2.2), the way of using the first order ABCs is straightforward. However, the situation is more complex if one wants to employ the second order ABCs. A direct substitution of (1.5) into (2.1) does not lead to a desirable result. To achieve the goal, we present a Lagrange multiplier approach.

First of all, we introduce a Lagrange multiplier $\Lambda = -\nabla\psi \cdot \mathbf{n}$ on the boundary Γ_A. In terms of Λ, we can rewrite the boundary integral as

$$-\int\limits_{\Gamma_A} \phi\nabla\psi \cdot \mathbf{n} \; d\Gamma_A = \int\limits_{\Gamma_A} \phi\Lambda \; d\Gamma_A. \tag{2.3}$$

Moreover, such a substitution gives the possibility to reformulate the ABCs (1.5) in the form

$$-\frac{1}{c}\dot{\Lambda} + \frac{1}{c^2}\ddot{\psi} - \frac{1}{2}\psi_{\tau\tau} = 0 \quad \text{on } \Gamma_A \times (0, t_n). \tag{2.4}$$

A weak formulation of (2.4) and following integration by parts yield

$$\int\limits_{\Gamma_A} \left(\left(-\frac{1}{c}\dot{\Lambda} + \frac{1}{c^2}\ddot{\psi} \right) \mu + \frac{1}{2}\psi_\tau\mu_\tau \right) d\Gamma_A - \frac{1}{2}\mu\psi_\tau \Big|_{\partial\Gamma_A} = 0 \quad \text{on } \Gamma_A \times (0, t_n), \tag{2.5}$$

for all test functions μ out of an appropriate Lagrange multiplier space. Besides, here $\partial\Gamma_A$ represents the endpoints of the boundary Γ_A.

Thus we have a system of two equations to be solved

$$\int\limits_{\Omega} \frac{1}{c^2}\ddot{\psi}\phi \; d\Omega + \int\limits_{\Omega} (\nabla\psi \cdot \nabla\phi) \, d\Omega + \int\limits_{\Gamma_A} \phi\Lambda \; d\Gamma_A = \int\limits_{\Gamma_E} \phi g \; d\Gamma_E \quad \text{in } \Omega \times (0, t_n), \tag{2.6a}$$

$$\int\limits_{\Gamma_A} \left(\left(-\frac{1}{c}\dot{\Lambda} + \frac{1}{c^2}\ddot{\psi} \right) \mu + \frac{1}{2}\psi_\tau\mu_\tau \right) d\Gamma_A - \frac{1}{2}\mu\psi_\tau \Big|_{\partial\Gamma_A} = 0 \quad \text{on } \Gamma_A \times (0, t_n). \tag{2.6b}$$

We start by discretizing (2.6a)-(2.6b) in space. For doing so, standard low order conforming finite elements are exploited while for ψ and Λ discrete Lagrange multiplier space satisfying a uniform inf-sup condition is used.

The discretized functions can be written in terms of nodal basis functions $N(\mathbf{x})$ within Ω and $N^{\Gamma_A}(\mathbf{x})$ on Γ_A as follows

$$\psi = \sum_{i=1}^{n} N_i(\mathbf{x})\psi_i,\ \phi = \sum_{j=1}^{n} N_j(\mathbf{x})a_j,\ \Lambda = \sum_{k=1}^{m} N_k^{\Gamma_A}(\mathbf{x})\lambda_k,\ \mu = \sum_{l=1}^{m} N_l^{\Gamma_A}(\mathbf{x})d_l. \tag{2.7}$$

Here n and m stand for internal and boundary nodes respectively. The substitution of (2.7) into system (2.6) leads to the following system of ordinary differential equations in time

$$\begin{aligned} &\int_{\Omega} \frac{1}{c^2} \sum_{i=1}^{n} N_i \ddot{\psi}_i N_j \ d\Omega + \int_{\Omega} \sum_{i=1}^{n} \nabla N_i \psi_i \cdot \nabla N_j \ d\Omega + \int_{\Gamma_A} N_j \sum_{k=1}^{m} N_k^{\Gamma_A} \lambda_k \ d\Gamma_A = \\ &\int_{\Gamma_E} N_j g \ d\Gamma_E,\ j = \overline{1,n} \quad \text{on } \Omega, \end{aligned} \tag{2.8a}$$

$$\begin{aligned} &\int_{\Gamma_A} \left(\left(-\frac{1}{c} \sum_{k=1}^{m} N_k^{\Gamma_A} \dot{\lambda}_k + \frac{1}{c^2} \sum_{i=1}^{n} N_i \ddot{\psi}_i \right) N_l^{\Gamma_A} + \frac{1}{2} \sum_{i=1}^{n} N_i' \psi_i \left(N_l^{\Gamma_A} \right)' \right) d\Gamma_A \\ &- \frac{1}{2} N_l^{\Gamma_A} \sum_{i=1}^{n} N_i' \psi_i \Big|_{\partial\Gamma_A} = 0, l = \overline{1,m} \quad \text{on } \Gamma_A \times (0, t_n). \end{aligned} \tag{2.8b}$$

The superscript prime indicates the tangential derivative. The algebraic formulation of problem (2.8) can be expressed as a semidiscrite system of linear ODEs

$$\begin{pmatrix} \mathbf{M} & 0 \\ \mathbf{B} & 0 \end{pmatrix} \begin{pmatrix} \ddot{\mathbf{\Psi}}^{n+1} \\ \ddot{\mathbf{\Lambda}}^{n+1} \end{pmatrix} + \begin{pmatrix} 0 & 0 \\ 0 & \mathbf{D} \end{pmatrix} \begin{pmatrix} \dot{\mathbf{\Psi}}^{n+1} \\ \dot{\mathbf{\Lambda}}^{n+1} \end{pmatrix} + \begin{pmatrix} \mathbf{K} & \widetilde{\mathbf{D}} \\ \widetilde{\mathbf{C}} & 0 \end{pmatrix} \begin{pmatrix} \mathbf{\Psi}^{n+1} \\ \mathbf{\Lambda}^{n+1} \end{pmatrix} = \begin{pmatrix} \mathbf{0} \\ \mathbf{0} \end{pmatrix}, \tag{2.9}$$

with the matrices

$$\begin{aligned} &\mathbf{M}_{ji} = \int_{\Omega} \frac{1}{c^2} N_i N_j \ d\Omega,\ \mathbf{K}_{ji} = \int_{\Omega} \nabla N_i \cdot \nabla N_j \ d\Omega, \\ &\mathbf{B}_{li} = \int_{\Gamma_A} \frac{1}{c^2} N_i N_l^{\Gamma_A} \ d\Gamma_A,\ \widetilde{\mathbf{D}}_{kl} = -\int_{\Gamma_A} N_k^{\Gamma_A} N_l^{\Gamma_A} \ d\Gamma_A. \end{aligned} \tag{2.10a}$$

$$\widetilde{\mathbf{C}}_{li} = \frac{1}{2} \left(\int_{\Gamma_A} (\nabla N_i \cdot \boldsymbol{\tau})(\nabla N_l^{\Gamma_A} \cdot \boldsymbol{\tau}) d\Gamma_A - N_i' N_l^{\Gamma_A} \Big|_{\partial\Gamma_A} \right),\ \mathbf{D}_{lk} = -\int_{\Gamma_A} \frac{1}{c} N_k^{\Gamma_A} N_l^{\Gamma_A} \ d\Gamma_A. \tag{2.10b}$$

Coupling between the acoustic field and second order ABC is accounted for by the submatrices $\mathbf{D}^{\mathrm{T}}$ and $\widetilde{\mathbf{C}}$.

2.2 The coupled field model

In the following derivation of the weak formulation we omit the time averaging of the term q and return to it later, at the stage of time discretization. In this part, we consider equations (1.1) and (1.2) coupled with the heat conduction equation (1.8).

We start from the weak formulation of the coupled ultrasonic heating problem taking into account the acoustic model with the temperature dependent speed of sound (1.1). The problem

reads as follows, find the maps $\psi(\cdot,t):\Omega\times(0,t_n)\to\mathbb{R}$ and $T(\cdot,t):\Omega\times(0,t_n)\to\mathbb{R}$ such that

$$\begin{aligned}&\int_\Omega c_\nu\rho(T)\dot{T}v\ d\Omega+\int_\Omega\kappa\left(\nabla T\cdot\nabla v\right)\ d\Omega-\int_\Omega\rho_0\left(\nabla\dot{\psi}\cdot\nabla\psi\right)v\ d\Omega\\&+\int_{\Gamma_A}\rho_0\dot{\psi}v\Lambda\ d\Gamma_A+\int_\Omega\rho_0\nabla\left(\dot{\psi}v\right)\cdot\nabla\psi\ d\Omega=0\quad\text{in }\Omega\times(0,t_n),\end{aligned}\tag{2.11a}$$

$$\int_\Omega c^{-2}(T)\ddot{\psi}\phi d\Omega+\int_\Omega\dot{\psi}\frac{\partial}{\partial t}c^{-2}(T)\phi d\Omega+\int_\Omega\left(\nabla\psi\cdot\nabla\phi\right)d\Omega+\int_{\Gamma_A}\phi\Lambda d\Gamma_A=0\quad\text{in }\Omega\times(0,t_n),\tag{2.11b}$$

$$\int_{\Gamma_A}\left(\left(-c^{-1}(T)\dot{\Lambda}+c^{-2}(T)\ddot{\psi}\right)\mu+\frac{1}{2}\psi_\tau\mu_\tau\right)d\Gamma_A-\frac{1}{2}\mu\psi_\tau\Big|_{\partial\Gamma_A}=0\text{ on }\Gamma_A\times(0,t_n).\tag{2.11c}$$

The weak formulation of the coupled ultrasound heating problem, based on equation (1.2), reads as follows. Find the maps $\psi(\cdot,t):\Omega\times(0,t_n)\to\mathbb{R}$ and $T(\cdot,t):\Omega\times(0,t_n)\to\mathbb{R}$ such that along with equation (2.11a) the following equations hold

$$\begin{aligned}&\int_\Omega\frac{1}{c^2}\ddot{\psi}\phi\ d\Omega+\int_\Omega\left(\nabla\psi\cdot\nabla\phi\right)\ d\Omega+\int_{\Gamma_A}\phi\Lambda\ d\Gamma_A+\int_{\Gamma_A}\frac{b}{c^2}\phi\dot{\Lambda}\ d\Gamma_A+\int_\Omega\frac{b}{c^2}\left(\nabla\dot{\psi}\cdot\nabla\phi\right)d\Omega-\\&\int_\Omega\frac{B}{A}\frac{1}{c^4}\ddot{\psi}\dot{\psi}\phi\ d\Omega-\int_\Omega\frac{2}{c^2}\left(\nabla\dot{\psi}\cdot\nabla\psi\right)\phi\ d\Omega=\int_{\Gamma_E}\phi g\ d\Gamma_E\quad\text{in }\Omega\times(0,t_n),\end{aligned}\tag{2.12a}$$

$$\int_{\Gamma_A}\left(\left(-\frac{1}{c}\dot{\Lambda}+\frac{1}{c^2}\ddot{\psi}\right)\mu+\frac{1}{2}\psi_\tau\mu_\tau\right)d\Gamma_A-\frac{1}{2}\mu\psi_\tau\Big|_{\partial\Gamma_A}=0\quad\text{on }\Gamma_A\times(0,t_n).\tag{2.12b}$$

Substituting the discretized functions (2.7) and

$$T=\sum_{p=1}^{n}N_p(\mathbf{x})T_p\,;\quad v=\sum_{q=1}^{n}N_q(\mathbf{x})v_q$$

into (2.11) and (2.12) results in the global semidiscrete system which can be expressed in matrix notation as

$$\begin{aligned}&\begin{pmatrix}0&0&0\\0&\mathbf{M}&0\\0&\mathbf{B}&0\end{pmatrix}\begin{pmatrix}\ddot{\mathbf{T}}^{n+1}\\\ddot{\mathbf{\Psi}}^{n+1}\\\ddot{\mathbf{\Lambda}}^{n+1}\end{pmatrix}+\begin{pmatrix}\mathbf{C}(\mathbf{T}^{n+1})&\mathbf{N}_3(\mathbf{\Psi}^{n+1})-\mathbf{N}_2(\mathbf{\Psi}^{n+1})+\mathbf{E}(\mathbf{\Lambda}^{n+1})&0\\0&\mathbf{Q}(\mathbf{T}^{n+1})&0\\0&0&\mathbf{D}\end{pmatrix}\begin{pmatrix}\dot{\mathbf{T}}^{n+1}\\\dot{\mathbf{\Psi}}^{n+1}\\\dot{\mathbf{\Lambda}}^{n+1}\end{pmatrix}+\\&\begin{pmatrix}\widetilde{\mathbf{K}}&0&0\\0&\mathbf{K}&\widetilde{\mathbf{D}}\\0&\widetilde{\mathbf{C}}&0\end{pmatrix}\begin{pmatrix}\mathbf{T}^{n+1}\\\mathbf{\Psi}^{n+1}\\\mathbf{\Lambda}^{n+1}\end{pmatrix}=\begin{pmatrix}\mathbf{0}\\\mathbf{f}\\\mathbf{0}\end{pmatrix}\end{aligned}\tag{2.13}$$

and

$$\begin{aligned}&\begin{pmatrix}0&0&0\\0&\mathbf{M}-\mathbf{N}_1(\dot{\mathbf{\Psi}}^{n+1})&0\\0&\mathbf{B}&0\end{pmatrix}\begin{pmatrix}\ddot{\mathbf{T}}^{n+1}\\\ddot{\mathbf{\Psi}}^{n+1}\\\ddot{\mathbf{\Lambda}}^{n+1}\end{pmatrix}+\begin{pmatrix}\mathbf{C}(\mathbf{T}^{n+1})&\mathbf{N}_3(\mathbf{\Psi}^{n+1})-\mathbf{N}_2(\mathbf{\Psi}^{n+1})+\mathbf{E}(\mathbf{\Lambda}^{n+1})&0\\0&\mathbf{K}_1-\widetilde{\mathbf{N}}_2(\mathbf{\Psi}^{n+1})&\mathbf{D}_1\\0&0&\mathbf{D}\end{pmatrix}\\&\times\begin{pmatrix}\dot{\mathbf{T}}^{n+1}\\\dot{\mathbf{\Psi}}^{n+1}\\\dot{\mathbf{\Lambda}}^{n+1}\end{pmatrix}+\begin{pmatrix}\widetilde{\mathbf{K}}&0&0\\0&\mathbf{K}&\widetilde{\mathbf{D}}\\0&\widetilde{\mathbf{C}}&0\end{pmatrix}\begin{pmatrix}\mathbf{T}^{n+1}\\\mathbf{\Psi}^{n+1}\\\mathbf{\Lambda}^{n+1}\end{pmatrix}=\begin{pmatrix}\mathbf{0}\\\mathbf{f}\\\mathbf{0}\end{pmatrix},\end{aligned}\tag{2.14}$$

with the right hand side

$$f_j = \int\limits_{\Gamma_E} N_j g \; d\Gamma_E, \tag{2.15}$$

and the following matrices

$$\mathbf{N}_1(\dot{\psi})_{ji} = \int\limits_{\Omega} \frac{1}{c^4}\frac{B}{A} N_i \sum_{k=1}^{n} N_k \dot{\psi}_k N_j \; d\Omega, \;\; \mathbf{N}_2(\psi)_{qi} = \int\limits_{\Omega} \rho_0 \left(\nabla N_i \cdot \nabla \sum_{k=1}^{n} N_k \psi_k \right) N_q \; d\Omega, \tag{2.16a}$$

$$\mathbf{N}_3(\psi)_{qi} = \int\limits_{\Omega} \rho_0 \left(\nabla \left(N_i N_q \right) \cdot \nabla \sum_{k=1}^{n} N_k \psi_k \right) \; d\Omega, \;\; \mathbf{E}(\lambda)_{qi} = \int\limits_{\Gamma_A} \rho_0 N_i N_q \sum_{k=1}^{m} N_k^{\Gamma_A} \lambda_k \; d\Gamma_A, \tag{2.16b}$$

$$\widetilde{\mathbf{K}}_{ji} = \int\limits_{\Omega} \kappa \nabla N_i \cdot \nabla N_j \; d\Omega, \;\; \mathbf{Q}_{ji}(T) = \int\limits_{\Omega} \frac{\partial}{\partial t} c^{-2}(T) N_i N_j \; d\Omega, \;\; \mathbf{C}(T)_{qp} = \int\limits_{\Omega} c_\nu \rho(T) N_p N_q d\Omega, \tag{2.16c}$$

$$\begin{aligned} \mathbf{K}_{1,ji} &= \int\limits_{\Omega} b c^{-2} \nabla N_i \cdot \nabla N_j \; d\Omega, \;\; \mathbf{D}_{1,lk} = -\int\limits_{\Gamma_A} b c^{-2} N_k^{\Gamma_A} N_l^{\Gamma_A} \; d\Gamma_A, \\ \widetilde{\mathbf{N}}_2(\psi)_{qi} &= \int\limits_{\Omega} 2c^{-2} \left(\nabla N_i \cdot \nabla \sum_{k=1}^{n} N_k \psi_k \right) N_q \; d\Omega. \end{aligned} \tag{2.16d}$$

The obtained systems of equations (2.13) and (2.14) are nonlinear and they can be solved by the Newton method, but if the time-averaged term q is taken into account and one intends to use multi-time stepping methods then we have to decouple the heat equation from the acoustic equation (2.11b). We do such a decoupling by applying a multi-time stepping method considered in the next section.

3 The multi-time stepping method

In the view of the fact that the heat transfer and wave propagation processes evolve in different time scales, we apply the multi-time stepping integration strategy to the solution of system (2.13). In this section, we propose a multi-time stepping scheme based on the fixed point iteration method and compare it with a similar non-iterative approach.

In order to approximate system (2.13) in time, we apply the generalized α-method [6] giving unconditional stability for the linear equations and quadratic order with respect to time. Thus we have

$$\dot{\mathbf{u}}^{n+1} = a_1 \mathbf{u}^{n+1} - \hat{\dot{\mathbf{u}}}^n, \quad \ddot{\mathbf{u}}^{n+1} = a_2 \mathbf{u}^{n+1} - \hat{\ddot{\mathbf{u}}}^n, \tag{3.1}$$

where

$$\hat{\dot{\mathbf{u}}}^n = a_1 \mathbf{u}^n + \frac{(1-\alpha_f)\gamma - \beta}{\beta} \dot{\mathbf{u}}^n + \frac{(1-\alpha_f)(\gamma - 2\beta)}{2\beta} \Delta t \ddot{\mathbf{u}}^n, \quad \hat{\ddot{\mathbf{u}}}^n = a_2 \mathbf{u}^n + \frac{1-\alpha_m}{\beta \Delta t} \dot{\mathbf{u}}^n + \frac{1-\alpha_m - 2\beta}{2\beta} \ddot{\mathbf{u}}^n,$$

and $\mathbf{u} = (T, \psi, \lambda)^{\mathrm{T}}$ while the parameters $a_1 = (1-\alpha_f)\gamma/(\beta \Delta t), \quad a_2 = (1-\alpha_m)/(\beta \Delta t^2)$.

Besides, we introduce some extra notations which will be needed throughout this section, namely $a_{1,\delta t} = (1-\alpha_f)\gamma/(\beta \delta t)$, $a_{2,\delta t} = (1-\alpha_m)/(\beta \delta t^2)$ with time step $m\delta t = \Delta t$ where Δt and δt are time steps for temperature elevation and wave propagation, respectively. It is assumed that Δt is an integer multiplier of $m\delta t$.

Keeping in mind the multi-rate integration idea [7, 9, 12, 15, 22, 23], we discretize system (2.13) in time by the generalized α-method that gives

$$\begin{pmatrix} 0 & 0 & 0 \\ 0 & a_{2,\delta t}\mathbf{M} & 0 \\ 0 & a_{2,\delta t}\mathbf{B} & 0 \end{pmatrix} \begin{pmatrix} \mathbf{T}^{n+1} \\ \mathbf{\Psi}^{n+\frac{1}{m}i} \\ \mathbf{\Lambda}^{n+\frac{1}{m}i} \end{pmatrix} + \begin{pmatrix} a_1\mathbf{C}(\mathbf{T}^{n+1}) & 0 & 0 \\ 0 & a_{1,\delta t}\mathbf{Q}(\mathbf{T}^{n+\frac{1}{m}i}) & 0 \\ 0 & 0 & a_{1,\delta t}\mathbf{D} \end{pmatrix} \begin{pmatrix} \mathbf{T}^{n+1} \\ \mathbf{\Psi}^{n+\frac{1}{m}i} \\ \mathbf{\Lambda}^{n+\frac{1}{m}i} \end{pmatrix} +$$

$$\begin{pmatrix} \widetilde{\mathbf{K}} & 0 & 0 \\ 0 & \mathbf{K} & \widetilde{\mathbf{D}} \\ 0 & \widetilde{\mathbf{C}} & 0 \end{pmatrix} \begin{pmatrix} \mathbf{T}^{n+1} \\ \mathbf{\Psi}^{n+\frac{1}{m}i} \\ \mathbf{\Lambda}^{n+\frac{1}{m}i} \end{pmatrix} = \begin{pmatrix} \mathbf{C}(\mathbf{T}^{n+1})\hat{\dot{\mathbf{T}}}^{n} + (\mathbf{N}_2(\mathbf{\Psi}^{n+1}) - \mathbf{N}_3(\mathbf{\Psi}^{n+1}) - \mathbf{E}(\mathbf{\Lambda}^{n+1}))\dot{\mathbf{\Psi}}^{n+1} \\ \mathbf{M}\hat{\ddot{\mathbf{\Psi}}}^{n+\frac{1}{m}(i-1)} + \mathbf{Q}(\mathbf{T}^{n+\frac{1}{m}i})\hat{\dot{\mathbf{\Psi}}}^{n+\frac{1}{m}(i-1)} \\ \mathbf{B}\hat{\dot{\mathbf{\Psi}}}^{n+\frac{1}{m}(i-1)} + \mathbf{D}\hat{\mathbf{\Lambda}}^{n+\frac{1}{m}(i-1)} \end{pmatrix},$$

$i = 1, 2, \ldots, m.$ (3.2)

To proceed with the solution of the nonlinear system (3.2), we reformulate it in a suitable manner for further application of Newton's iteration

$$\mathbf{F}(\mathbf{T}^{n+1}, \mathbf{\Psi}^{n+\frac{1}{m}i}, \mathbf{\Lambda}^{n+\frac{1}{m}i}) = 0,\ i = 1, 2, \ldots, m, \tag{3.3}$$

with the corresponding left hand side omitted here for short. The Newton method for equation (3.3) is

$$\mathbf{F}'(\mathbf{T}^{n+1}, \mathbf{\Psi}_k^{n+\frac{1}{m}i}, \mathbf{\Lambda}_k^{n+\frac{1}{m}i})\Delta\mathbf{X} = -\mathbf{F}(\mathbf{T}^{n+1}, \mathbf{\Psi}_k^{n+\frac{1}{m}i}, \mathbf{\Lambda}_k^{n+\frac{1}{m}i}), \tag{3.4}$$

where $\mathbf{F}'$ stands for the Jacobian with respect to the variables $\mathbf{T}^{n+1}$, $\mathbf{\Psi}^{n+\frac{1}{m}i}$, $\mathbf{\Lambda}^{n+\frac{1}{m}i}$, and $\Delta\mathbf{X} = (\Delta\mathbf{T}, \Delta\mathbf{\Psi}, \Delta\mathbf{\Lambda})^{\mathrm{T}}$. For the Newton method, we are allowed to chose any updating scheme for the Jacobian. In this work, we use the full Newton method, i.e. the Jacobian is performed at each iteration, demonstrating excellent convergence behavior.

Algorithm 1 The multi-time stepping scheme based on the fixed point iteration method

Set up matrices $\mathbf{M}$, $\mathbf{B}$, $\mathbf{D}$, $\widetilde{\mathbf{K}}$, $\mathbf{K}$, $\widetilde{\mathbf{D}}$, $\widetilde{\mathbf{C}}$ and initial conditions for the model.
for all time steps n=0,1,2,... **do**
  for all fixed point iteration steps $k = 1, 2, \ldots, k_{\max}$ **do**
    for all inner time steps i=1,2,...,m **do**
      Compute $T_{k-1}^{n+\frac{1}{m}i} = \left(1 - \frac{i-1}{m}\right) T_{k-1}^{n} + \frac{i-1}{m} T_{k-1}^{n+1}$.
      Solve nonlinear system (3.2) with respect to $\psi_k^{n+\frac{1}{m}i}$ and $\Lambda_k^{n+\frac{1}{m}i}$.
      Update $\dot{\psi}_k^{n+\frac{1}{m}i}$, $\ddot{\psi}_k^{n+\frac{1}{m}i}$ and $\dot{\Lambda}_k^{n+\frac{1}{m}i}$, $\ddot{\Lambda}_k^{n+\frac{1}{m}i}$.
    end for
    Compute $\langle q \rangle = \sqrt{\frac{1}{m}\sum_{j=1}^{m} q_j^2 \left(\psi_k^{n+\frac{1}{m}i}\right)}$.
    Solve system (3.2) with respect to T_k^{n+1}.
    Check for fixed point iteration convergence, i.e.
    $\frac{\|\mathbf{u}_k - \mathbf{u}_{k-1}\|}{\|\mathbf{u}_k\|} \le \varepsilon, \quad \mathbf{u}_k = \left(T_k^{n+1}, \psi_k^{n+1}, \Lambda_k^{n+1}\right)$.
  end for
end for

The essence of Algorithm 1 is to solve equation (2.11b) with ABC (2.11c) at a constant temperature field. In a second step, we compute $\langle q \rangle$ and solve the heat equation (2.11a) and the acoustic model with the interpolated temperature afterwards. This iterative process continues until the solution converges. The non-iterative Algorithm 2 is completely analogous to its counterpart save for the absence of the fixed point iteration method that implies $k_{\max} = 1$. We use this algorithm to solve the coupled system (2.12). The question concerning stability analysis of the methods for the considered problem remains to be answered in the forthcoming research.

4 Numerical computations

In this section, firstly the linear (1.7) and nonlinear (1.2) wave equations are verified. Secondly, we compare the ABC used and validate our approach concerning the applicability of the second order ABC in the weak formulation. Further, the linear coupled field model are examined, and then the fixed point iteration and non-iterative methods are compared for the nonlinear coupled model. In the closing part, we present some numerical results for the ultrasound heating problem.

4.1 Verification of wave propagation

This section starts with the examination of how linear and non-linear acoustic waves travel in an open vertical tube of air. We consider a two-dimensional tube of length $L = 1.0$m and width 0.2m with the ABC of second order set on top. On the side boundaries of the tube, homogeneous Neumann boundary conditions are applied. At the bottom boundary, a monofrequency transducer producing waves of the form $\sin(2\pi 10^3 t)$ is set. The speed of sound is taken to be $c = 343\text{m}\cdot\text{s}^{-1}$, and $B/A = 0.4$, $b = 5.5 \cdot 10^{-13}$. For the simulations, the time step is $1.25 \cdot 10^{-5}$s while the diameter of the element is $h = \{0.05, 0.025, 0.0125\}$. The exact solution is set to $\psi(y,t) = \sin(2\pi 10^3 (tc - y)/c)$ for both linear (1.7) and non-linear (1.2) wave equations.

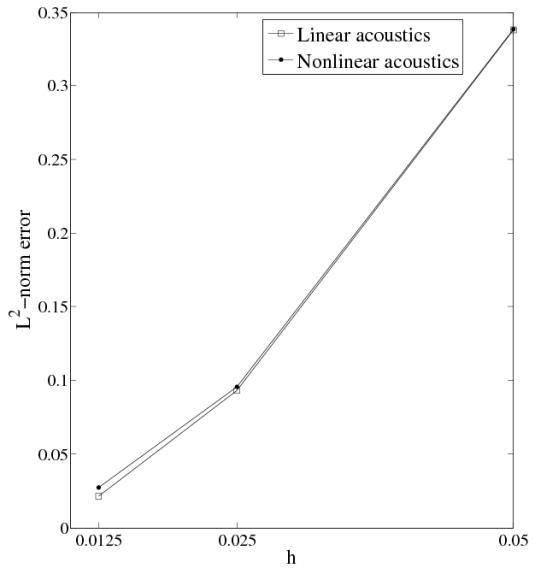

Figure 2: L^2-norm error averaged over time for linear and nonlinear wave propagations using different h.

As it is seen in Fig. 2, the L^2-norm error decreases with mesh refinement pointing out the convergence of the solution for linear as well for non-linear regimes of wave propagation.

To continue we consider another test case and evaluate the wave response to changing in its frequency. Let us have a horizontal two-dimensional tube of length $L = 10$m and width 1m closed at the right end. On the top and bottom boundaries, homogeneous Neumann boundary conditions are applied. An acoustic wave of the form $\sin(2\pi\omega t)$ is emitted from the left boundary. All the other parameters are set the same as in previous case except for the time step and the diameter of the element which are $1.25 \cdot 10^{-4}$s and 0.125m respectively.

As it is known [5], an approximated fundamental wave frequency at which acoustic resonance occurs in the closed tube is given by the expression $f_{\text{res}} = c/(4L)$. For our case, the fundamental resonance frequency is 8.575Hz. In Fig. 3, the linear and nonlinear waves propagation are shown for the waves with different frequencies: a subresonance at frequency $f = 6.0$Hz (I.a) and resonance (II.a) cases.

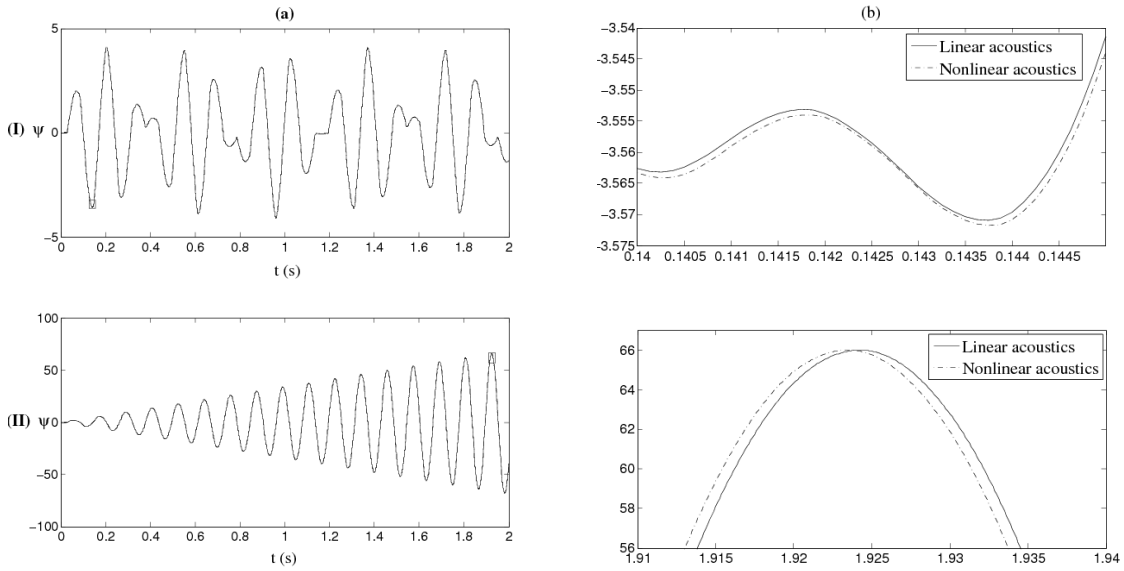

Figure 3: Linear and nonlinear acoustic wave propagation in a closed tube of air: a) **(I)** – subresonance and **(II)** – resonance cases for the point with coordinates $(10.0, 0.5)$. b) Zoomed display to see the difference between the linear and nonlinear computations.

Fig. 3 shows that both the subresonance and resonance cases give almost the same results which are in good agreement with theoretical predictions.

4.2 A comparison between the first and second order ABCs for linear waves

In spite of the importance of effective ABCs, there still exists a bit of confusion about what kind of non-reflecting boundary conditions provide the best result in the given problem. In this section, we compare the first and second order Engquist–Majda ABCs.

The example presented in Fig. 4 consists of a tube with the right wall inclined at an angle of 45 degrees to the horizontal axis. There is a monochromatic sinusoidal source emitting waves at a frequency of 1kHz on the left wall whereas the homogeneous Neumann boundary conditions are set on the horizontal walls. As it can be seen from Fig. 4, the distortions of the incoming waves due to the reflected waves spawn by the imperfection of the ABCs are much higher for the first order ABC. Furthermore, the simulation illustrates that the proposed technique of using Lagrange multipliers as a bridge between the weak formulation of the original problem and the second order ABC is valid and efficient. From now on, we use the second order ABC in all the forthcoming simulations.

4.3 The linear coupled field model

Here, we concentrate on the comparison of our numerical computations with an analytical solution of a simple setup. We solve for the linear coupled model, consisting of the linear wave (1.7) and the heat conduction (1.8) equations with constant density. We consider the same problem setup and the exact solution as for the linear wave equation above. The exact solution to equation (1.8) with $\rho = const$ and a homogeneous Dirichlet boundary value problem set on all the boundaries can be found in [3].

Fig. 5 shows that the error decreases as the mesh is refined. Moreover, the increase in time step ratio has virtually no influence on the accuracy of the results. The latter allows to use much

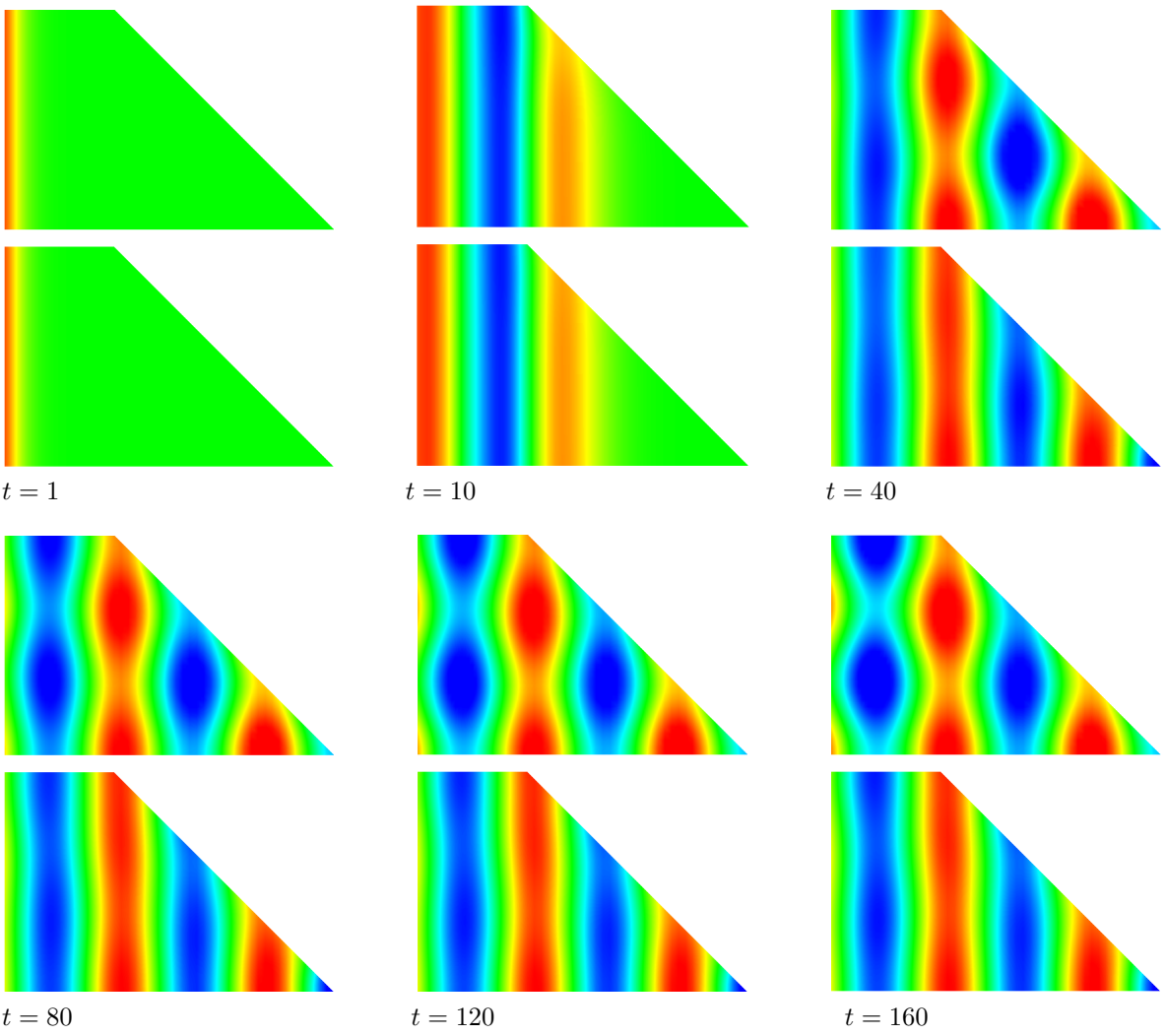

Figure 4: The influence of the first (above) and second (below) order ABCs set on the sloping side of a 2D domain upon acoustic waves propagated from left to right. A series of snapshots after 1, 10, 40, 80, 120 and 160 time steps.

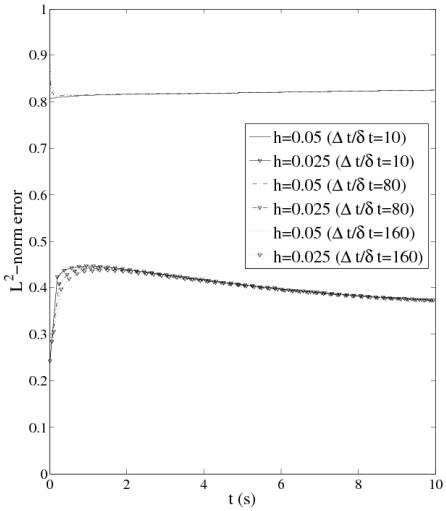

Figure 5: L^2-norm error as a function of time for the linear coupled model using different time step ratios $\Delta t/\delta t$ and h.

bigger time steps for the heat conduction equation in comparison with the acoustic one that in turn leads to substantially faster execution times.

4.4 Comparison of the fixed point iteration and non-iterative methods

In this part, we make some experiments to compare the performance of the proposed methods. Throughout this section we use the same problem setup as in Sec. 4.5. Furthermore, the tolerance of the fixed point iteration is $\varepsilon = 10^{-10}$, and the number of iterations per time step is 2.

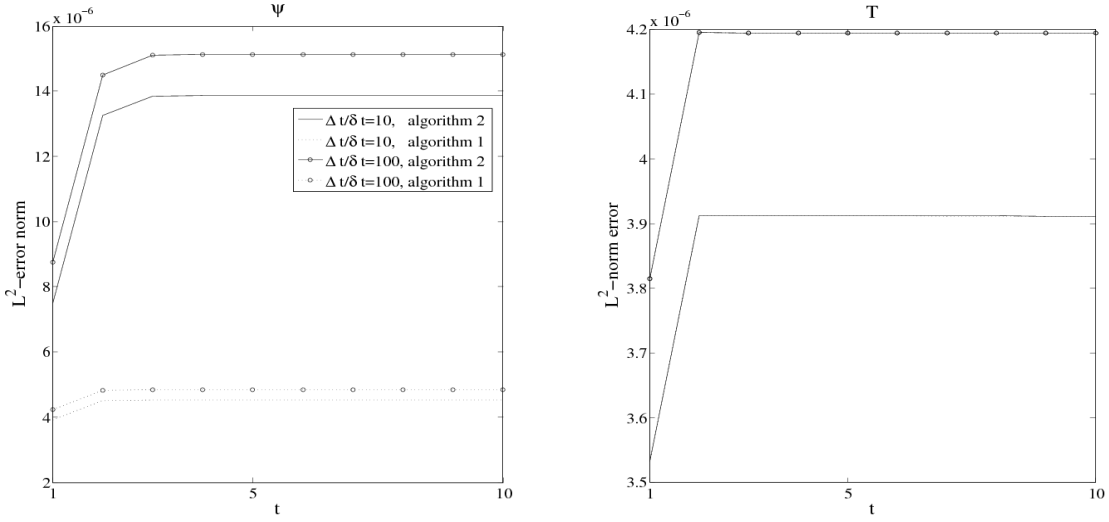

Figure 6: L^2-norm error at different time steps ratios for the coupled model (2.11) versus time: the acoustic potential (left) and the temperature field (right).

As Fig. 6 demonstrates, the fixed point iteration scheme (Algorithm 1) performs slightly better for the wave propagation and gives virtually no difference for the heat conduction compared to

Algorithm 2. However, Algorithm 1 is at least twice as expensive as Algorithm 2, and thus Algorithm 2 is more efficient.

We also applied Algorithm 2 to the coupled model (2.12). Figure 7 illustrates that the error

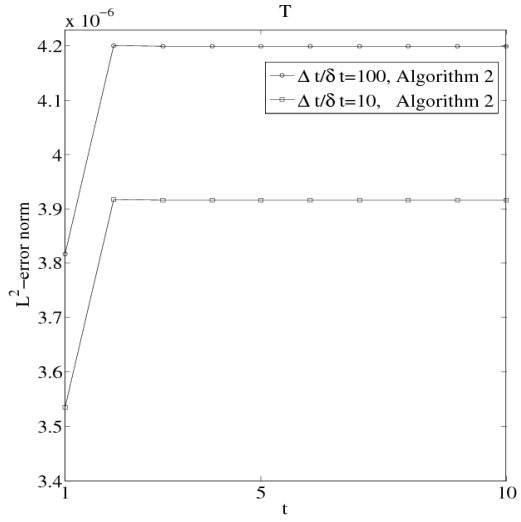

Figure 7: L^2-norm error at different time steps ratios for the coupled model (2.12) versus time.

grows very slowly compared to the ratio of time steps. We do not show the error for the acoustic potential since it is always zero. Basing on these and other numerical experiments, we can conclude that the proposed algorithm can be applied to the numerical solution of the coupled nonlinear problem (2.12), and it proposes a substantial improvement in the performance.

4.5 The ultrasound heating problem

The description of the numerical simulation of heat transferring for the model (2.11) we begin with introducing a computational domain $\Omega = [0, 0.02\text{m}] \times [0, 0.04\text{m}]$ and an equidistant quadrilateral finite element mesh with an element diameter $0.15625 \cdot 10^{-3}$m. The simulation domain Ω is divided into two equal subdomains $\Omega_F = [0, 0.02\text{m}] \times [0, 0.02\text{m}]$, $\Omega_T = [0, 0.02\text{m}] \times [0.02\text{m}, 0.04\text{m}]$.

Within each of the subdomains, different temperature dependencies for the density and the speed of sound are used:

PROBLEM PARAMETERS

liquid domain	target material
$\rho(T) = \rho_i/(1.0 + \beta(T - T_0))$	$\rho = const,\ K = const$
$c(T) = \sqrt{K/\rho(T)}$	$c = \sqrt{K/\rho}$

Here K is the bulk modulus of the corresponding media, ρ_i and T_0 are initial values of the density and the temperature distributions and β is the volumetric temperature expansion coefficient of the fluid.

The wave transducer located at the bottom of the domain emits sinusoidal acoustic waves at a frequency of 1MHz and with an amplitude 0.12 traveling from bottom to top. That implies inhomogeneous Neumann boundary conditions

$$\frac{\partial \psi}{\partial \mathbf{n}} = -0.12 \sin(2\pi 10^6 t) \quad \text{on } \Gamma_E \times [0, t_n]. \tag{4.1}$$

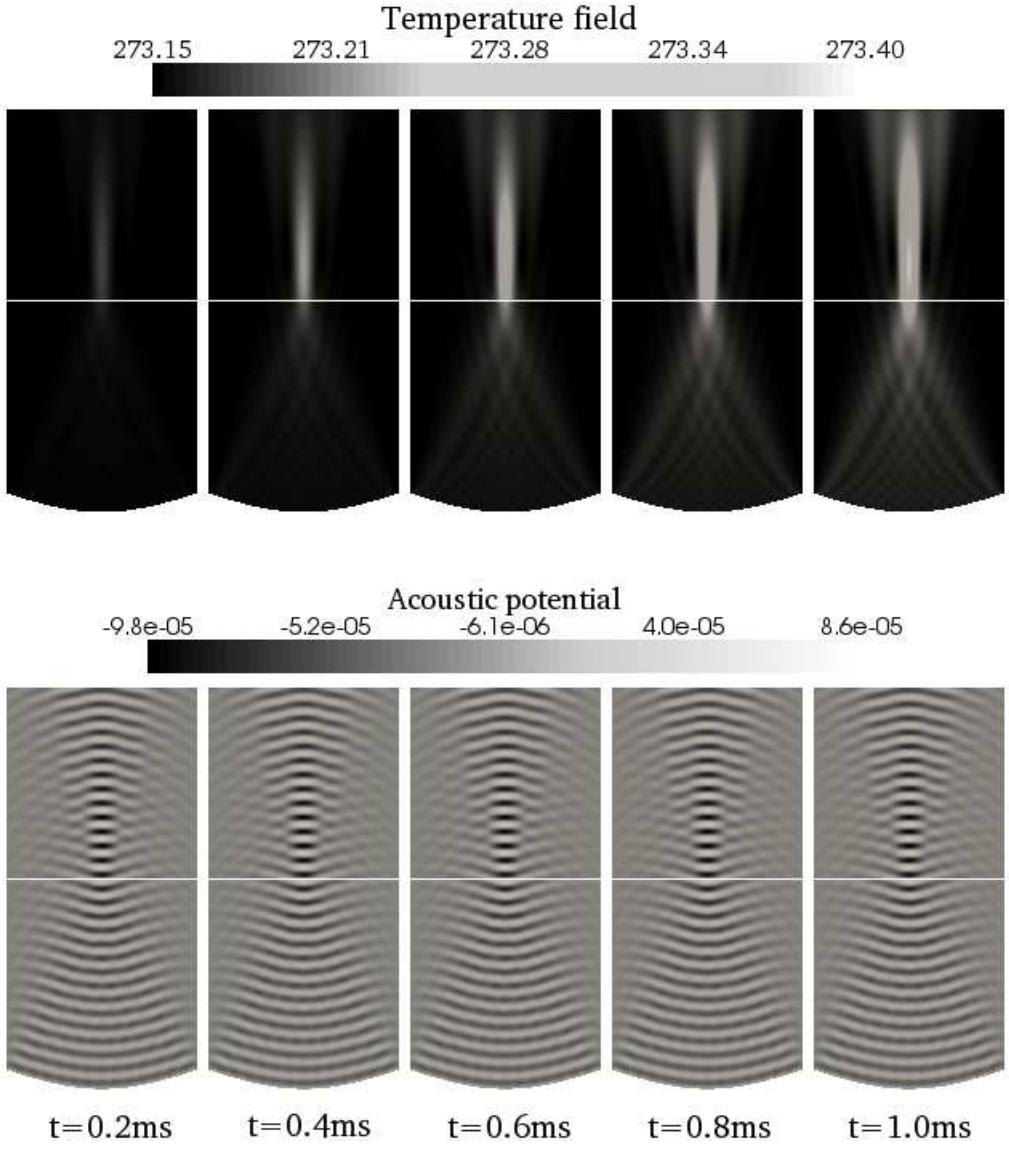

Figure 8: A series of snapshots after 0.2 ms, 0.4 ms, 0.6 ms, 0.8 ms and 1.0 ms of insonation. The evolution of the temperature and acoustic fields.

We set the second order Engquist–Majda ABCs on all the boundaries save for the bottom one whereas the temperature field is set to 273.15K on all the boundaries.

Fig. 8 shows a series of snapshots, taken every 0.2 ms, of the evolution of the temperature and acoustic fields for the domain Ω divided into two subdomains: tissue – upper region and fluid – lower region. We also did numerical simulations for model (2.12) and found out that taking into account the distortion in the speed of sound due to the temperature in the time scales used in the ultrasonic heating problem does not reveal a substantial disparity in the temperature field compared to problem (2.11).

References

[1] R. J. Astley. Transient wave envelope elements for wave problems. *J. Sound Vibration*, 192(1):245–261, 1996.

[2] J. P. Bérenger. A perfectly matched layer for the absorption of electromagnetic waves. *J. Comput. Phys.*, 114(2):185–200, 1994.

[3] H. S. Carslaw and J. C. Jaeger. *Conduction of heat in solids*. Oxford University Press, 1996.

[4] T.J. Cavicchi and W.D. Jr. O'Brien. Heat generation by ultrasound in an absorbing medium. *The Journal of the Acoustical Society of America*, 76(4):1244–1245, 1984.

[5] D. Chattopadhyay and P.C. Rakshit. *Elements of Physics Vol. I.* New Age Publications, 2004.

[6] J. Chung and G.M. Hulbert. A time integration algorithm for structural dynamics with improved numerical dissipation - the generalized *alpha*-method. *J. Appl. Mech.*, 60(2):371–375, 1993.

[7] J. Donea and H. Laval. Nodal partition of explicit finite element methods for unsteady diffusion problems. *Comput. Methods Appl. Mech. Engrg.*, 68(2):189–204, 1988.

[8] B. B. Engquist and A. Majda. Absorbing boundary conditions for the numerical simulation of waves. *Math. Comp.*, 31(139):629–651, 1977.

[9] Ch. Engstler and Ch. Lubich. Multirate extrapolation methods for differential equations with different time scales. *Computing*, 58(2):173–185, 1997.

[10] D. Givoli. High-order local non-reflecting boundary conditions: a review. *Wave motion*, 39(4):319–326, 2004.

[11] D. Givoli and B. Neta. High-order non-reflecting boundary conditions for dispersive waves. *Wave Motion*, 37(3):257–271, 2003.

[12] T. Hughes and W. K. Liu. Implicit-explicit finite elements in transient analysis: Implementation and numerical examples. *J. Appl. Mech.*, 45(2):375–378, 1978.

[13] J.B. Keller and D. Givoli. Exact non-reflecting boundary conditions. *J. Comput. Phys.*, 82(1):172–192, 1989.

[14] V.I. Kuznetsov. Equations of nonlinear acoustics. *Soviet Physics-Acoustics*, 16(4):467–470, 1971.

[15] W. K. Liu and T. Belytschko. Mixed-time implicit-explicit finite elements for transient analysis. *Computers & Structures*, 15(4):445–450, 1982.

[16] S. Makarov and M. Ochmann. Nonlinear and thermoviscous phenomena in acoustics, part i. *Acta Acustica united with Acustica*, 82(4):579–606, 1996.

[17] S. Makarov and M. Ochmann. Nonlinear and thermoviscous phenomena in acoustics, part ii. *Acta Acustica united with Acustica*, 83(2):197–222, 1997.

[18] S. Marburg and B. Nolte. *Computational acoustics of noise propagation in fluids: finite and boundary element methods*. Springer, 2008.

[19] K. Naugolnykh and L. Ostrovsky. *Nonlinear Wave Processes in Acoustics*. Cambridge University Press, 1998.

[20] W.L. Nyborg. Heat generation by ultrasound in a relaxing medium. *J. Acoust. Soc. Am.*, 70(2):310–312, 1981.

[21] H.H. Pennes. Analysis of tissue and arterial blood temperature in the resting human forearm. *The Journal of Applied Physiology*, 1(2):93–122, 1948.

[22] P. Smolinski. An explicit multi-time step integration method for second order equations. *Comput. Methods Appl. Mech. Engrg.*, 94(1):25–34, 1992.

[23] P. Smolinski, T. Belytschko, and M. Neal. Multi-time-step integration using nodal partitioning. *Internat. J. Numer. Methods Engrg.*, 26(2):349–359, 1988.

M. Kaltenbacher
Alps-Adriatic University of Klagenfurt
Universitätsstrasse 65-67
A-9020 Klagenfurt
Austria

I. Shevchenko
Institute for Applied Analysis and Numerical Simulation
Pfaffenwaldring 57
D-70569 Stuttgart
Germany

B. Wohlmuth
Institute for Applied Analysis and Numerical Simulation
Pfaffenwaldring 57
D-70569 Stuttgart
Germany

Erschienene Preprints ab Nummer 2010/001

Komplette Liste: `http://preprints.ians.uni-stuttgart.de`

2010/001 *Kaltenbacher, M., Shevchenko, I., Wohlmuth, B. I.:* Investigation of heat generation by acoustic waves